

Observation of geometric phases for three-level systems using NMR interferometry

Hongwei Chen,¹ Mingguang Hu,² Jingling Chen,² and Jiangfeng Du^{1,*}

¹*Hefei National Laboratory for Physical Sciences at Microscale and Department of Modern Physics, University of Science and Technology of China, Hefei, Anhui 230026, People's Republic of China*

²*Theoretical Physics Division, Chern Institute of Mathematics, Nankai University, Tianjin 300071, People's Republic of China*

(Received 7 May 2008; published 10 November 2009)

Inspired by the optical experimental scheme [Phys. Rev. Lett. **86**, 369 (2001)], we propose and implement a NMR experiment to observe an Abelian geometric phase shift arising from the cyclic evolution of U(2)-invariant states. Such a phase shift geometrically refers to the Bargmann invariant in a four-dimensional SU(3)/U(2) parameter space, while the usual geometric phases arise in the evolution of U(1)-invariant states and is related to solid angles in a two-dimensional SU(2)/U(1) $\approx S^2$ parameter space (or Poincaré sphere). We present the experiment in a four-level system and investigate its topological invariance for different circuits. This may provide a realistic candidate to design complex geometric quantum circuits for future quantum computers.

DOI: [10.1103/PhysRevA.80.054101](https://doi.org/10.1103/PhysRevA.80.054101)

PACS number(s): 03.65.Vf, 76.60.-k

I. INTRODUCTION

Cyclic evolution can enable a nondegenerate state to acquire geometric phase (GP) factors [1] that depend only on the geometry of the state in its parameter space. If the cyclic variation is adiabatic, this GP is known as Berry's phases [2]. Otherwise it is related to Aharonov-Anandan phases [3], which has been pointed out to be a continuous version of earlier Pancharatnam phases [4]. The geometric phase is important not only for its fundamental interests but also for its potential usages. Due to the independence of energy and time and relying only on the geometry in the parameter space, GP is argued to be resilient to certain types of errors and suggest the possibility of an intrinsically fault-tolerant way of performing quantum gate operations [5,6].

Experimental observation of GP, so far, has exclusively concentrated on the Abelian geometric phase arising in the evolution of U(1)-invariant states [7–12]. These states can be for instance a two-level state parameterized by a polar angle and an azimuth angle in the Poincaré sphere. The GP of it corresponds to a solid angle subtended by closed evolution paths on the sphere. This geometric property of GP is the main concern in experiment before. But when considering in a three-level system, things will become different and interesting. A general state in this system resides on a four-dimensional SU(3)/U(2) parameter space and its GP for the cyclic evolution has been studied theoretically [13,14,16]. It is found that GP in the three-level ray space is geometrically referred to the Bargmann invariant [15–17] on a hypersurface instead of the solid angle on a sphere. Unitary evolution in it belongs to the SU(3) group operation that provides more controllable parameters than that of SU(2) does in the two-level case. All these substantially provide more choices for designing complex geometric quantum circuits [18,19]. Although it is well known in theory what is lacking is an experimental to observe three-level GP in any physical system. To this aim, precise controlling operation is needed. NMR system happens to have mature techniques of controlling operation, and therefore it seems to be one of the best physical systems to carry out this experiment.

In this paper inspired by the optical experimental scheme [20], we propose and implement a NMR experiment to observe an Abelian GP, which arises from geodesic transformations of U(2)-invariant states in a four-dimensional SU(3)/U(2) parameter space. Four levels generated by two interacting spin-1/2 nuclei are exploited to contribute three target levels and one auxiliary level. Unitary evolutions, belonging to SU(3), for performing cyclic paths in the three-dimensional ray space are implemented by using quantum controlled logic gates [21]. Aimed at obtaining a measurable GP, we utilize the auxiliary level to be as a reference state that is kept unchanged during all evolutions. The dynamical phase factor can be vanished by evolving along geodesics in the projective Hilbert space. As a result, an observable geometric phase factor appears as a local phase between the three-level target state and the reference state.

II. GEOMETRIC PHASE OF THREE-LEVEL SYSTEMS

Let us begin by considering a three-level Hilbert space \mathcal{H}^3 and an arbitrary three-component state can be characterized by four real parameters $(\alpha_1, \alpha_2, \chi_1, \chi_2)$ besides a trivial global phase parameter η ,

$$|\psi\rangle = e^{i\eta}(e^{i\chi_1} \cos \alpha_1, e^{i\chi_2} \sin \alpha_1 \cos \alpha_2, \sin \alpha_1 \sin \alpha_2)^T. \quad (1)$$

The real parameters have the range $\alpha_{1,2} \in [0, \pi/2]$ and $\chi_{1,2} \in [0, 2\pi)$. These parameters are independent and form a four-dimensional parameter space. Although it cannot directly draw a four-dimensional geometry for illustration, we can respectively view (α_1, α_2) as points on an octant of S^2 and (χ_1, χ_2) on a torus (see Fig. 1). By doing this, we should remember that only the combination of these two geometrical spaces determines the parameter space in consideration, which is indicated by using a Kronecker product in Fig. 1. Now, consider a state evolving from $|\psi(s_1)\rangle$ to $|\psi(s_2)\rangle$ and curve parameters $s_{1,2}$ consisting of the five parameters defined in Eq. (1). Corresponding to this evolution, in \mathcal{H}^3 there is a continuous piecewise smooth parametrized curve, $C = \{|\psi(s)\rangle | s_1 \leq s \leq s_2\}$, and its image in the ray space \mathcal{R} is likewise continuous and piecewise smooth denoted by $\mathcal{C} = \{\rho(s) = |\psi(s)\rangle\langle\psi(s)| | s_1 \leq s \leq s_2\}$. Then the GP β associated with the curve \mathcal{C} equals the difference between a total phase φ_{tot} and a dynamical phase γ_d [14], that is,

*djf@ustc.edu.cn

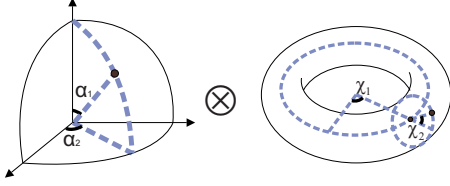


FIG. 1. (Color online) An illustration of the four-dimensional Hilbert space. We can visually image it as the direct product \otimes of two two-dimensional surfaces, one octant (α_1, α_2) of a sphere S^2 and a torus (χ_1, χ_2). Their coordinate parameters are marked in the figure.

$$\beta[C] = \varphi_{\text{tot}}[C] - \gamma_d[C], \quad \varphi_{\text{tot}}[C] = \arg\langle \psi(s_1) | \psi(s_2) \rangle,$$

$$\gamma_d[C] = - \int_{s_1}^{s_2} ds \langle \psi(s) | i \frac{\partial}{\partial s} | \psi(s) \rangle, \quad (2)$$

with both φ_{tot} and γ_d being functionals of the curve C . If the curve C is closed, the state change can be simply expressed as $|\psi(s_2)\rangle = \exp\{i(\gamma_d[C] + \beta[C])\} |\psi(s_1)\rangle$.

The geodesics in ray space \mathcal{R} are given through variations in a nondegenerate positive-definite length functional; see details in [16]. In two-level systems geodesics are related to the parallel transport condition. But for the three-level case, every geodesic in ray space has a vanishing geometric phase and it plays a crucial role in the observation of geometric phases in the following. The simplest description of geodesic can always be achieved as follows [14]. Let ρ_k and ρ_{k+1} denote the end points of a smooth curve C associated with unit vectors ψ_k and ψ_{k+1} in \mathcal{H}^3 . There is a requirement for the chosen state vectors that $\langle \psi_k | \psi_{k+1} \rangle$ must be real positive. Then the geodesic C_{geo} connecting ρ_k to ρ_{k+1} is the ray space image of the curve $C_{\text{geo}} = \{\psi(s_k) | 0 \leq s_k \leq s_k^0\}$ and

$$\psi(s_k) = \psi_k \cos s_k + \frac{\psi_{k+1} - \psi_k \langle \psi_k | \psi_{k+1} \rangle}{\sqrt{1 - \langle \psi_k | \psi_{k+1} \rangle^2}} \sin s_k, \quad (3)$$

with $0 \leq s_k \leq s_k^0$ and $s_k^0 = \arccos\langle \psi_{k+1} | \psi_k \rangle$. From Eq. (3), one can see that $\psi(0) = \psi_k$ and $|\psi(s_k^0)\rangle \langle \psi(s_k^0)| = |\psi_{k+1}\rangle \langle \psi_{k+1}| = \rho_{k+1}$. For a set of points $\rho_1, \rho_2, \dots, \rho_n \subset \mathcal{R}$ in order, suppose that no two consecutive points are mutually orthogonal and that ρ_n and ρ_1 are also nonorthogonal. So we can obtain a closed curve C in \mathcal{R} in the form of an n -sided polygon by joining these n points cyclically with geodesic arcs. The geometric phase is then according to Eq. (2)

$$\beta[C] = \arg\langle \psi_1 | \psi'_1 \rangle - \arg\langle \psi_1 | \psi_2 \rangle - \dots - \arg\langle \psi_n | \psi'_1 \rangle$$

$$= - \arg \text{Tr}(\rho_1 \rho_2 \dots \rho_n), \quad (4)$$

in which it has used relations of $|\psi'_1\rangle \langle \psi'_1| = |\psi_1\rangle \langle \psi_1| = \rho_1$ and $\rho_1^2 = \rho_1$. Equation (4) combined with geodesic condition, i.e., $\langle \psi_k | \psi_{k+1} \rangle$ is real positive, shows a vanishing dynamical phase for these cyclic evolutions. It thus provides us a convenient evolution way to observe the geometric phase.

III. EXPERIMENTS

Experiments were performed on the three-dimensional subspace of two interacting spin- $\frac{1}{2}$ nuclei—spin a (^1H) and

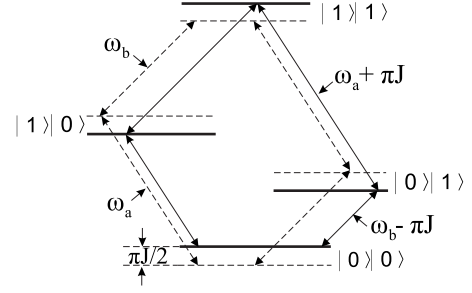


FIG. 2. Energy level diagram for (solid lines) two spins coupled by a Hamiltonian of the form of $2\pi\hbar J_z^a I_z^b$ and (dashed lines) two uncoupled spins.

spin b (^{13}C) in the ^{13}C -labeled chloroform molecule CHCl_3 . The reduced Hamiltonian for this two spin system is, to an excellent approximation, given by $H = \omega_a I_z^a + \omega_b I_z^b + 2\pi J I_z^a I_z^b$. The first two terms in the Hamiltonian describe the free precession of spin a and spin b around the magnetic field B_0 with Larmor frequencies $\omega_a/2\pi \approx 400$ MHz and $\omega_b/2\pi \approx 100$ MHz. The third term of the Hamiltonian describes a scalar spin-spin coupling of the two spins with $J = 214.5$ Hz. ^{13}C nucleus's T_1 relaxation time is 17.2 s and its T_2 relaxation time is 0.35 s. ^1H nucleus's T_1 relaxation time is 4.8 s and its T_2 relaxation time is 3.3 s. Experiments were performed at room temperature on a Bruker AV-400 spectrometer. If we denote the spin up and down by $|0\rangle$ and $|1\rangle$, the energy levels of such system are displayed in Fig. 2. It has four levels written as $\{|00\rangle, |01\rangle, |10\rangle, |11\rangle\}$ corresponding to energy eigenvalues $\{\frac{1}{2}\hbar(-\omega_1 - \omega_2 + \pi J), \frac{1}{2}\hbar(-\omega_1 + \omega_2 - \pi J), \frac{1}{2}\hbar(\omega_1 - \omega_2 - \pi J), \frac{1}{2}\hbar(\omega_1 + \omega_2 + \pi J)\}$. We choose basis states $\{|00\rangle, |10\rangle, |11\rangle\}$ to construct the desired three-level space \mathcal{H}^3 and $|01\rangle$ as the reference state which is kept unchanged during evolutions.

The system was first prepared in a pseudopure state $|00\rangle$ using the method of spatial averaging [22] with the pulse sequence

$$R_x^b(\pi/3) \rightarrow G_z \rightarrow R_x^b(\pi/4) \rightarrow 1/2J \rightarrow R_y^b(\pi/4) \rightarrow G_z,$$

which is read from left to right (as the following sequences). The rotations $R_{\text{axis}}^{\text{spins}}(\text{angle})$ are implemented by radio-frequency pulses. G_z is a pulsed field gradient which destroys all coherences (x and y magnetizations) and retains longitudinal magnetization (z magnetization component) only. $\frac{1}{2J}$ represents a free precession period of the specified duration under the coupling Hamiltonian.

The complete sequence for state evolutions started by preparing the initial superposition state $\frac{1}{\sqrt{2}}(|00\rangle + |01\rangle)$ with a Hadamard operation on the second qubit of the pseudopure state $|00\rangle$. Then the reference term $|01\rangle$ was kept unchanged through bipartite control operations. The $|00\rangle$ term (denoted by $|\psi_1\rangle$) was first evolved to $|\psi_2(s_1)\rangle = \cos s_1 |00\rangle + \sin s_1 |10\rangle$ with unitary operation $U_1^a(s_1) |\psi_1\rangle \rightarrow |\psi_2(s_1)\rangle$, then to state $|\psi_3(s_2)\rangle = (\cos s_1^0 \cos s_2 - e^{i\varphi} \sin s_1^0 \sin s_2 \cos \theta) |00\rangle + (\sin s_1^0 \cos s_2 + e^{i\varphi} \cos s_1^0 \sin s_2 \cos \theta) |10\rangle - \sin \theta \sin s_2 |11\rangle$ with $U_2^b(s_2) |\psi_2(s_1^0)\rangle \rightarrow |\psi_3(s_2)\rangle$, and last to state $|\psi'_1\rangle = e^{i\beta} |\psi_1\rangle$ with $U_3^a(s_3^0) |\psi_3(s_2^0)\rangle \rightarrow |\psi'_1\rangle$. The experimental network has been shown in Fig. 3. In order to show the evolving path obviously, here we have written the states and their evolution

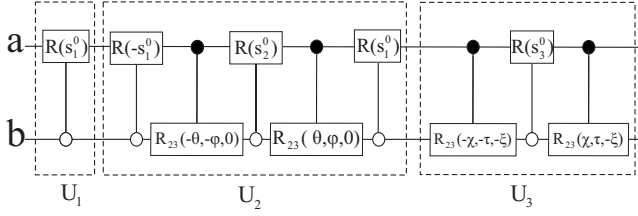


FIG. 3. Experimental network: two spin-1/2 nuclei perform unitary evolutions controlled by each other. Each circle at the second line means that spin-1/2 nuclei performs its linked unitary evolution when the second nucleus at $|0\rangle_b$ state. Each dot at the first line means that spin-1/2 nuclei performs its linked unitary evolution when the first nucleus at $|1\rangle_a$ state.

operations in a curve-parameter form. The curve parameters $s_{1,2,3}$ take values from 0 to $s_{1,2,3}^0$, respectively. Corresponding to three smooth geodesics, the unitary operations can be factored into more clear forms,

$$U_1^g(s_1) = R(s_1),$$

$$U_2^g(s_2) = R(s_1^0)R_{23}(\theta, \varphi, 0)R(s_2)R_{23}^{-1}(\theta, \varphi, 0)R^{-1}(s_1^0),$$

$$U_3^g(s_3) = R_{23}(\chi, \tau, -\xi)R(-s_3)R_{23}^{-1}(\chi, \tau, -\xi), \quad (5)$$

where the controlled rotation quantum gates have the form

$$R(s_k) = \begin{pmatrix} \cos s_k & 0 & -\sin s_k & 0 \\ 0 & 1 & 0 & 0 \\ \sin s_k & 0 & \cos s_k & 0 \\ 0 & 0 & 0 & 1 \end{pmatrix},$$

$$R_{23}(\vartheta, \phi_t, \phi_r) = \begin{pmatrix} 1 & 0 & 0 & 0 \\ 0 & 1 & 0 & 0 \\ 0 & 0 & e^{i\phi_t} \cos \vartheta & e^{-i\phi_r} \sin \vartheta \\ 0 & 0 & -e^{i\phi_r} \sin \vartheta & e^{-i\phi_t} \cos \vartheta \end{pmatrix}.$$

The concrete experimental realization for these quantum gates is discussed at last. Parameters ξ , χ , τ , and s_3^0 in Eq. (5) are fixed by the reparameterization, $|\psi_3\rangle = e^{i\xi} \cos s_3^0 |00\rangle + e^{i(\xi+\chi)} \sin s_3^0 \cos \tau |10\rangle - \sin s_3^0 \sin \tau |11\rangle$. Obviously the chosen unit vectors ψ_k and ψ_{k+1} satisfy the condition of $\langle \psi_k | \psi_{k+1} \rangle$ being real positive. This combined with Eq. (4) shows a vanishing dynamical phase during these cyclic evolutions and we obtain the GP

$$\beta[C] = \arg(\cos s_1^0 \cos s_2^0 - e^{i\varphi} \sin s_1^0 \sin s_2^0 \cos \theta). \quad (6)$$

So after one cyclic evolution described above, it effectively produces a GP and can be measured as a relative phase shift between $|0\rangle_b$ and $|1\rangle_b$ for the qubit b , i.e., $\frac{1}{\sqrt{2}}(|00\rangle + |01\rangle) \rightarrow \frac{1}{\sqrt{2}}(e^{i\beta}|00\rangle + |01\rangle) \rightarrow |0\rangle_a \otimes \frac{1}{\sqrt{2}}(e^{i\beta}|0\rangle + |1\rangle)_b$. At last the local phase β can be read out directly by a phase-sensitive detector on qubit b in NMR.

Though it is hard to image how a state evolves in a high-dimensional Hilbert space, here we would take an example to explain this. If we set the unitary operation parameters as $s_1 = \pi/2$, $s_2 = \pi/4$, $\theta = \pi/4$, and $\varphi = \pi/4$, there are four steps in the following for a cyclic evolution: (i) The evolution begins with an initial state $|\psi_1\rangle = |00\rangle$ or $|\psi_1\rangle = (1, 0, 0)^T$,

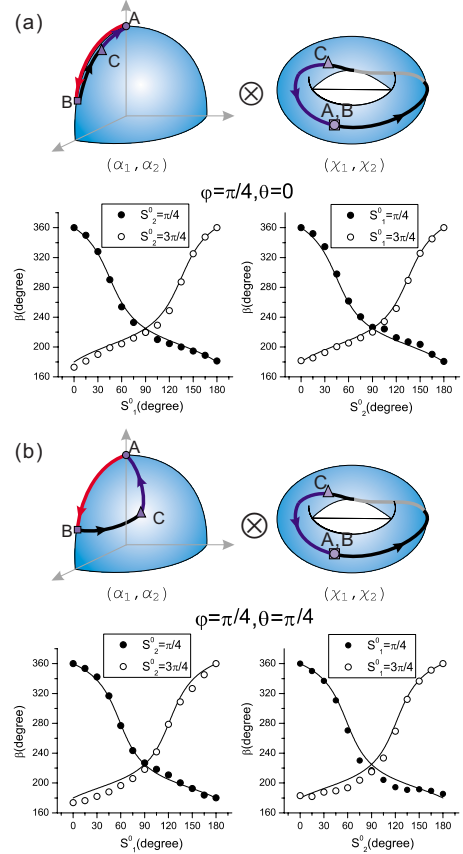


FIG. 4. (Color online) Experimental results on the GP β versus the parameter s_1^0 or s_2^0 . Changing s_1^0 , s_2^0 means changing the positions of states $|\psi_2$ (point B) and $|\psi_3$ (point C). The evolution paths have been depicted out illustratively in parameter space (a direct product manifold of an octant of sphere S^2 and a torus) and the concrete values of $(\alpha_1, \alpha_2, \chi_1, \chi_2)$ can be calculated by Eq. (1). (a) shows the result in the cases of $\theta=0$ and $\varphi=\pi/4$; the evolution path A-B-C on the octant of S^2 is a curve while it runs a period on the torus. (b) shows the result in the cases of $\theta=\pi/4$ and $\varphi=\pi/4$; the evolution A-B-C on the octant of S^2 is a triangle while it runs a period on the torus. Theoretical curves for GP have been marked out by solid lines.

which in comparison with Eq. (1) actually defines a point A with $(\alpha_1 = \alpha_2 = \chi_1 = \chi_2 = 0)$ in the parameter space. (ii) A unitary operation U_1 drives the state vector from $|\psi_1\rangle$ to $|\psi_2\rangle$ [$|\psi_2\rangle = (\cos(s_1), \sin(s_1), 0)^T$]. Compared with Eq. (1), the state $|\psi_2\rangle$ defines a point B with $(\alpha_1 = \pi/2, \alpha_2 = \chi_1 = \chi_2 = 0)$ in the parameter space. So in octant, the vector moves from point A ($\alpha_1 = \alpha_2 = 0$) to B ($\alpha_1 = \pi/2, \alpha_2 = 0$), while in the torus parameter space, the point A ($\chi_1 = \chi_2 = 0$) coincides with B ($\chi_1 = \chi_2 = 0$). (iii) A unitary operation U_2 drives the state vector from $|\psi_2\rangle$ to $|\psi_3\rangle$ [$|\psi_3\rangle = -(0.3536 + 0.3536i, -0.707, 0.5)^T$]. In the parameter space, $|\psi_3\rangle$ can be expressed as a point C with $(\alpha_1 = \pi/3, \alpha_2 = 0.6155)$ and $(\chi_1 = \pi/4, \chi_2 = \pi)$. (iv) A unitary operation U_3 drives the state vector $|\psi_3\rangle$ back to the start point A with an extra phase β , which is nothing but the three-level geometric phase of a cyclic evolution. In the above description, we have omitted the energy level $|01\rangle$ because it is the reference level which is kept unchanged during evolutions.

In Fig. 4 we show the measured phase β versus param-

eters $\{s_1^0, s_2^0, \theta, \varphi\}$ that are determined by evolution states ψ_1 (point A), ψ_2 (point B), and ψ_3 (point C). All are carried out at $\varphi = \pi/4$, and total pulse sequence time T for cyclic evolution is about 5–25 ms for different evolution paths. We set $\theta = 0$ and $\theta = \pi/4$, respectively, at which correspondent geodesics have disparate trajectories in ray space. The measured phase is in all cases seen to fit the theoretical curve [Eq. (6)] well with a root-mean-square deviation across all data sets of 5.6° . Thus, all results are in close agreement with the predicted geometric phase, and it is clear that we are able to accurately control the amount of phase geometrically. The total experimental time of ~ 18 ms was short compared to the shortest relaxation time T_2 of ~ 350 ms. The sign decay during evolution progress is less than 5%, and this will not effect the measurement of geometric phase shift. The experiment errors are mostly due to errors in the rotation angles of the radio-frequency pulse, which arise from the inhomogeneity of the radio-frequency field.

The controlled operation between the two qubits plays the main role in the experiment. It goes as that the qubit a (or b) undergoes a SU(2) operation if the qubit b (or a) is in state $|1\rangle$ while kept unchanged if it is in state $|0\rangle$. This is used to realize the controlled operations R and R_{23} . The detailed operations in experiment work as follows.

For the subsystem of qubit a , we can write the reduced Hamiltonian

$$H_a = \omega_a I_z^a + 2\pi J m_z^b I_z^a = [\omega_a - 2\pi J(d^b - 1/2)] I_z^a,$$

where m_z^b is the eigenvalue of I_z^b ($= \pm \frac{1}{2}$) and d^b the corresponding computational value ($= 0, 1$). If we use a rotating frame with a frequency of $\omega'_a = \omega_a$ and $\omega'_b = \omega_b$, the Hamiltonian turns into, for $d^b = 0$, $H_a^{(0)} = \pi J I_z^a$, while it becomes $H_a^{(1)} = -\pi J I_z^a$ for $d^b = 1$. This Hamiltonian generates controlled rotations around the z axis. Qubit b is the control qubit and qubit a is the target qubit. To generate the control gate $R(S_k)$, we rotate the rotation axis using radio-frequency pulses. To generate a $2S_k$ rotation around the y -axis, e.g., we use the sequence

$$R_x^a(\pi/2) \rightarrow \frac{S_k}{\pi J} \rightarrow R_x^a(-\pi/2) \rightarrow R_y^a(S_k).$$

This represents the controlled gate operation $R(S_k)$.

For another controlled gate operation $R_{23}(\chi, \tau, -\xi)$, we have to reverse the roles of control and target qubit and apply the following sequence to qubit b :

$$\begin{aligned} R_z^b(-\phi') \rightarrow R_y^b(-\pi - \beta') \rightarrow \frac{\alpha'}{2\pi J} \rightarrow R_y^b(\pi + \beta') \\ \rightarrow R_z^b(\phi') \rightarrow R_n^b(\alpha'/2, \beta', \phi'), \end{aligned}$$

$R_n^b(\alpha'/2, \beta', \phi')$ denote the rotation of the second qubit $\alpha'/2$ around the axis $\vec{n}(\beta', \phi')$, and α' , β' , and ϕ' are calculated from χ , τ , and $-\xi$.

IV. CONCLUSION

In summary, we present the first experiment for producing and measuring an Abelian SU(3)/U(2) geometry-dependent phase shift in a three-level system. Although the increased dimensions in parameter space complicate the analysis of unitary evolution, we succeed in designing a scheme in control by using NMR techniques. In a two interacting qubits system, it provides naturally three target levels that are used to perform cyclic evolution and an auxiliary level that is kept unchanged to create a reference state. Thus an easily measurable geometric phase factor appears as a local phase factor. Obviously our experiment by using NMR techniques turns out to be more feasible than the optical scheme proposed in Ref. [20]. It should be noted that our operations adopted may be readily extended to perform the geometric quantum gates as proposed in [18,19]. If some new geometric quantum circuits are developed based on the SU(3)/U(2) geometry, our experimental scheme also serves as a realistic candidate.

ACKNOWLEDGMENTS

This work was supported by the National Science Foundation for Postdoctoral Scientists, the National Natural Science Foundation of China, the CAS, and the National Fundamental Research Program 2007CB925200. J.-L.C. acknowledges support in part by the NSF of China (Grant No. 10975075), the Program for New Century Excellent Talents in University, and the project sponsored by SRF for ROCS, SEM.

-
- [1] J. Anandan, Nature (London) **360**, 307 (1992).
 - [2] M. V. Berry, Proc. R. Soc. London, Ser. A **392**, 45 (1984).
 - [3] Y. Aharonov and J. Anandan, Phys. Rev. Lett. **58**, 1593 (1987).
 - [4] S. Pancharatnam, Proc. Indian Acad. Sci., Sec. A **44**, 247 (1956).
 - [5] J. A. Jones *et al.*, Nature (London) **403**, 869 (2000).
 - [6] D. Leibfried *et al.*, Nature (London) **422**, 412 (2003).
 - [7] T. Bitter and D. Dubbers, Phys. Rev. Lett. **59**, 251 (1987).
 - [8] A. Tomita and R. Y. Chiao, Phys. Rev. Lett. **57**, 937 (1986).
 - [9] D. Suter *et al.*, Phys. Rev. Lett. **60**, 1218 (1988).
 - [10] J. F. Du *et al.*, Phys. Rev. Lett. **91**, 100403 (2003).
 - [11] J. F. Du *et al.*, Phys. Rev. A **76**, 042121 (2007).
 - [12] P. J. Leek *et al.*, Science **318**, 1889 (2007).
 - [13] G. Khanna *et al.*, Ann. Phys. **253**, 55 (1997).
 - [14] Arvind *et al.*, J. Phys. A **30**, 2417 (1997).
 - [15] V. Bargmann, J. Math. Phys. **5**, 862 (1964).
 - [16] N. Mukunda and R. Simon, Ann. Phys. **228**, 205 (1993).
 - [17] R. Simon and N. Mukunda, Phys. Rev. Lett. **70**, 880 (1993).
 - [18] Xiang-Bin Wang and M. Keiji, Phys. Rev. Lett. **87**, 097901 (2001); **88**, 179901(E) (2002).
 - [19] S. L. Zhu and Z. D. Wang, Phys. Rev. Lett. **89**, 097902 (2002).
 - [20] B. C. Sanders *et al.*, Phys. Rev. Lett. **86**, 369 (2001).
 - [21] L. M. K. Vandersypen and I. L. Chuang, Rev. Mod. Phys. **76**, 1037 (2005).
 - [22] D. G. Cory *et al.*, Physica D **120**, 82 (1998).